Theoretical study of the interaction of carbon monoxide with $3d$ metal dimers

Ling Jiang, and Qiang Xu

Citation: The Journal of Chemical Physics **128**, 124317 (2008); doi: 10.1063/1.2842066
View online: https://doi.org/10.1063/1.2842066
View Table of Contents: http://aip.scitation.org/toc/jcp/128/12
Published by the American Institute of Physics

Theoretical study of the interaction of carbon monoxide with 3*d* metal dimers

Ling Jiang and Qiang Xu[a)]
National Institute of Advanced Industrial Science and Technology (AIST), Ikeda, Osaka 563-8577, Japan

(Received 10 December 2007; accepted 17 January 2008; published online 31 March 2008)

The interaction of carbon monoxide with 3*d* metal dimers (scandium through zinc) has been examined using six different exchange-correlation density functionals. Results are compared to the relevant experimental values and to other theoretical investigations when available, and the overall agreement has been obtained. The BP86 functional gives calculated C–O stretching vibrational frequencies much closer to the experimental values than the B3P86, B3LYP, mPW1PW91, and PBE1PBE functionals, and furthermore, replacing the correlation part by the Lee–Yang–Parr correlation functional yields essentially the same results. It is generally found that on going from left to right across the 3*d* metal series, the preference for geometrical configuration is from side-on-bonded mode to bridging, and then to terminal, whereas Ni_2CO adopts bridging mode. Particularly, the present computation reveals a significant tendency toward four-electron donor carbonyl groups with metal-oxygen bonds with the early transition metals scandium and titanium. The C–O stretching vibrational frequencies in the ground states of M_2CO (M=Sc to Zn) increase generally from the left to the right side of the Periodic Table. The binding energies exhibit an overall decrease trend. These general trends in the interaction of carbon monoxide with 3*d* metal dimers mirror the main features of CO adsorption on transition metal surfaces. © *2008 American Institute of Physics*. [DOI: 10.1063/1.2842066]

I. INTRODUCTION

The study of the interaction of carbon monoxide with transition metals is a topic of considerable interest from an academic or an industrial viewpoint.[1] Many industrial processes such as hydroformylation, Fischer–Tropsch synthesis, and acetic acid synthesis employ carbon monoxide as the reagent and transition metal compounds as heterogeneous or homogeneous catalysts and involve transition metal carbonyl intermediates.[2] Generally, the CO adsorption on the 3*d* metal surfaces of Sc to Fe indicate a tendency toward CO dissociation, whereas for Co to Cu, it tends to remain adsorbed on the surfaces.[1–8] In particular, unusually low C–O stretching frequencies around 1100–1400 cm^{-1} were observed on the Cr(110) and Fe(100) surfaces.[4] Weak adsorption of CO was observed on the Ni(111), Cu(111), Cu(110), and Cu(100) surfaces.[5–8]

Interest of the interaction of carbon monoxide with metal dimers remains high because it serves as the simplest model systems for fundamental understanding of the multifaceted mechanisms of carbon monoxide activation by metal clusters and surfaces. Recently, the reactions of CO with group 3 metal and early lanthanide dimers generated a new series of the $M_2[\eta^2(\mu_2\text{-C,O})]$ (M=Sc,Y,La,Ce,Gd) molecules with asymmetrically bridging and side-on-bonded CO ligands, which are drastically activated with remarkably low C–O stretching frequencies.[9–12] Matrix investigations of the reaction of some 3*d* metal dimers with CO molecules characterized a series of dinuclear carbonyls, Ti_2CO,[13] Mn_2CO,[14,15] Fe_2CO,[16–18] Co_2CO,[19] and Cu_2CO.[20] Theoretical investigations have been carried out for Fe_2CO,[21] Ni_2CO,[22] and Cu_2CO.[23–25] To explore the trends in the interaction of carbon monoxide with 3*d* metal dimers, systematical computations were carried out for the equilibrium geometries and harmonic vibrational frequencies of the possible structures and electronic states of M_2CO (M=Sc to Zn) with six popular density functionals in this study. Comparison with the relevant experimental values and with other theoretical investigations when available is also presented.

II. THEORETICAL METHODS

The GAUSSIAN 03 program was used for all calculations.[26] The 6-311+G(*d*) basis set was used for C and O atoms,[27] and the Wachters–Hay all-electron basis set was used for 3*d* metal atoms.[28,29] The functionals used in the present study have been denoted BP86, B3P86, BLYP, B3LYP, mPW1PW91, and PBE1PBE. The first four are constructed using either the pure density functional theory (DFT) exchange functional of 1988 (B) (Ref. 30) or the three-parameter Hartree–Fock/DFT hybrid exchange functional (B3) (Ref. 31) combined with the correlation functional of Perdew 86 (P86) (Refs. 32 and 33) or Lee–Yang–Parr (LYP).[34] The mPW1PW91 functional comprises modified Perdew–Wang exchange (mPW) and Perdew–Wang 1991 correlation (PW91).[35] The PBE1PBE functional consists of 25% exchange and 75% correlation weighting of 1997 hybrid functional of Perdew–Burke–Ernzerhof (PBE).[36] Considering that the BP86 and BPW91 (Refs. 30

a)Author to whom correspondence should be addressed. Electronic mail: q.xu@aist.go.jp.

TABLE I. Comparison of experimental and theoretical C-O stretching vibrational frequencies (cm^{-1}) for the ground state M_2CO (M=Sc to Zn) species. Parenthetical values are the deviations from the experimental values.

Species	State	BP86	B3P86	BLYP	B3LYP	mPW1PW91	PBE1PBE	Expt.
Sc_2CO	$^1A'$	1237.6	1291.2	1215.2	1271.9	1297.3	1300.5	1193.4[a]
		(44.2)	(97.8)	(21.8)	(78.5)	(103.9)	(107.1)	
Ti_2CO	$^3A''$	1330.9	1362.3	1313.9	1345.0	1364.3	1366.2	1297.8[b]
		(33.1)	(64.5)	(16.1)	(47.2)	(66.5)	(68.4)	
V_2CO	$^3A'$	1825.4	1932.6	1835.0	1936.0	2025.8	1826.2	1801.6[c]
		(23.8)	(131.0)	(33.4)	(134.4)	(224.2)	(24.6)	
Cr_2CO	$^1A'$	1947.3	2048.3	1944.0	2043.6	2057.3	2055.8	1879.1[c]
		(68.2)	(169.2)	(64.9)	(165.4)	(178.2)	(176.7)	
Mn_2CO	$^9A''$	1763.5	1822.8	1754.2	1809.0	1815.0	1814.4	
		(75.3)	(134.6)	(66.0)	(120.8)	(126.8)	(126.2)	1688.2[d]
		(76.0)	(135.3)	(66.7)	(121.5)	(127.5)	(126.9)	1687.5[e]
Fe_2CO	$^7A'$	1927.3	2051.2	1920.5	2038.0	2072.6	2070.6	1898.0[f]
		(29.3)	(153.2)	(22.5)	(140.0)	(174.6)	(172.6)	
Co_2CO	$^5A''$	1958.3	2109.5	1944.9	2098.5	2140.1	2100.1	1953.3[g]
		(5.0)	(156.2)	(−8.4)	(145.2)	(186.8)	(146.8)	
Ni_2CO	$^1A_1$	1793.0	1895.3	1773.6	1874.2	1909.1	1910.0	1769.1[c]
		(23.9)	(126.2)	(4.5)	(105.1)	(140.0)	(140.9)	
Cu_2CO	$^1\Sigma^+$	2071.1	2201.0	2055.1	2186.3	2223.7	2222.1	
		(−46.2)	(83.7)	(−62.2)	(69.0)	(106.4)	(104.8)	2117.3[c]
		(−44.9)	(85.0)	(−60.9)	(70.3)	(107.7)	(106.1)	2116[h]
Zn_2CO	$^1A'$	2120.8	2225.3	2112.2	2211.9	2242.3	2240.7	···

[a]Reference 9.
[b]Reference 13.
[c]Unpublished results of this laboratory.
[d]Reference 14.
[e]Reference 15.
[f]Reference 18.
[g]Reference 19.
[h]Reference 20.

and 37) functionals usually yield essentially the same results as were found in many cases such as metal carbonyls,[38,39] BPW91 was not used here. The equilibrium geometries and harmonic vibrational frequencies of the possible structures and electronic states of M_2CO (M=Sc to Zn) were calculated using the above-mentioned six density functionals. Molecular orbitals were generated with GAUSSVIEW.

III. RESULTS AND DISCUSSION

Table I reports the comparison of experimental and theoretical C–O stretching vibrational frequencies for the ground state M_2CO (M=Sc to Zn) species. It can be found from Table I that the BP86 and BLYP functionals give calculated C–O stretching vibrational frequencies much closer to the experimental values than the B3P86, B3LYP, mPW1PW91, and PBE1PBE functionals, and furthermore, the BP86 functional performs slightly better than the BLYP functional. Hereafter, mainly BP86 results are presented for discussion. Ground electronic states, point groups, vibrational frequencies, and intensities of the ground state M_2CO (M=Sc to Zn) species are listed in Table II. Calculated and experimental adiabatic ionization energies of the naked 3d metal dimers are given in Table III. Mulliken atomic charges of the ground state M_2CO (M=Sc to Zn) species are presented in Table IV. Figures 1–7 show representatively low-lying structures and their relative energies of M_2CO. Molecular orbital depictions of the highest occupied molecular orbitals (HOMOs) and HOMO-1s of the ground state M_2CO (M=Sc to Zn) species are illustrated in Fig. 8. All the configurations are found to be planar. The geometry optimization procedures starting with nonplanar trial structures without imposing any symmetry constraint all resulted in the planar configurations. Results of the present computations together with relevant experimental and previous theoretical work are presented below for each individual species, moving from left to right across the series.

A. Sc_2CO

The ground state of Sc_2CO is predicted to be $^1A'$ (Fig. 1), which has an asymmetrically bridging and side-on-bonded CO ligand. The $^3A'$ and $^5A'$ states of Sc_2CO lie 12.9 and 26.3 kcal/mol higher in energy than its ground state, respectively, and also present side-on-bonded configurations. The low-lying $^3B_2$ and $^5B_2$ states of Sc_2CO are above its ground state by 28.3 and 33.6 kcal/mol, respectively, corresponding to the structures with the CO molecules in the bridging position between the two scandium atoms. The lowest energy state with linear arrangement of atoms, $^1\Sigma^+$, lies 45.5 kcal/mol in energy higher than the $^1A'$ one. It is noted that the spin multiplicity of Sc_2 (the ground state is $^5\Sigma_u^-$) changes upon attachment of CO.

The C–O stretching vibrational frequency of the ground state of Sc_2CO is calculated to be 1237.6 cm^{-1}, which is consistent with the experimental value (1193.4 cm^{-1}) (Table I) and previous calculations.[9] The C–O bond length (1.321 Å) is much longer than the value of the free CO molecule (1.140 Å) calculated at the same level of theory, implying that the C–O bond is highly activated in this side-on-bonded Sc_2CO species. The Sc–Sc bond length in Sc_2CO is elongated by 0.111 Å relative to the naked Sc_2. The Sc–C

TABLE II. Ground electronic states, point groups, vibrational frequencies (cm^{-1}), and intensities (km/mol) of the ground state M_2CO (M=Sc to Zn) species calculated at the BP86/6-311+G(d) level of theory.

Species	Ground electronic state	Point group	Frequencies (intensity, mode)
Sc_2CO	$^1A'$	C_s	1237.6 (290,A'), 663.3 (1,A'), 546.7 (15,A'), 429.0 (19,A'), 338.4 (9,A''), 219.5 (3,A')
Ti_2CO	$^3A''$	C_s	1330.9 (303,A'), 719.1 (3,A'), 544.8 (2,A'), 367.1 (2,A''), 360.5 (6,A''), 256.7 (5,A'')
V_2CO	$^3A'$	C_s	1825.4 (888,A'), 672.5 (20,A'), 454.0 (0.2,A'), 421.0 (35,A'), 331.3 (2,A''), 84.4 (0.3,A')
Cr_2CO	$^1A'$	C_s	1947.3 (884,A'), 710.6 (35,A'), 399.1 (0.1,A'), 328.0 (21,A'), 288.8 (1,A''), 102.6 (5,A')
Mn_2CO	$^9A''$	C_s	1763.5 (612,A'), 507.4 (5,A'), 354.7 (3,A''), 321.5 (4,A'), 230.2 (1,A'), 107.2 (1,A')
Fe_2CO	$^7A'$	C_s	1927.3 (1213,A'), 462.2 (27,A'), 334.5 (4,A'), 301.5 (0.1,A''), 259.1 (23,A'), 51.3 (1,A')
Co_2CO	$^5A''$	C_s	1958.3 (1012,A'), 500.8 (20,A'), 364.8 (2,A''), 348.7 (5,A'), 292.1 (2,A'), 69.5 (1,A')
Ni_2CO	$^1A_1$	C_{2v}	1793.0 (498,A_1), 595.4 (0.1,B_2), 533.8 (0.01,A_1), 393.6 (5,B_1), 266.4 (0.4,A_1), 234.3 (1,B_2)
Cu_2CO	$^1\Sigma^+$	$C_{\infty v}$	2071.1 (668,σ), 425.8 (0.01,σ), 285.6 (6×2,π), 236.4 (4,σ), 33.1 (0.4×2,π)
Zn_2CO	$^1A'$	C_s	2120.8 (80,A'), 52.7 (0,A'), 15.4 (0.1,A'), 9.3 (0.1,A''), 8.6 (0.0001,A'), 2.5 (0.0001,A')

and Sc–O stretching frequencies are predicted to be 663.3, 546.7, and 429.0 cm^{-1} (Table II), respectively, while their intensities (1, 15, and 19 km/mol) are too small to be detected. The Sc–Sc stretching is predicted to be 219.5 cm^{-1} with small intensity (3 km/mol), which is beyond our spectral range of 5000–400 cm^{-1}.[9]

B. Ti_2CO

The ground state of Ti_2CO is predicted to be $^3A''$ and the geometrical configuration is similar to that of the ground state of Sc_2CO, where CO is also side-on bonded to the two titanium atoms (Fig. 2). Energetically next two higher structures of Ti_2CO with side-on-bonded configurations are calculated to be $^1A'$ and $^5A''$, respectively, which lie 8.5 and 13.5 kcal/mol higher in energy than its ground state. Two low-lying bridging configurations correspond to the $^5A_2$ and $^3A_2$ states, respectively, which are above its ground state by 16.1 and 21.4 kcal/mol. The lowest energy terminal configuration with an $^3A''$ state lies 29.6 kcal/mol higher in energy than its ground state. The present computations indicate that the spin multiplicity of Ti_2 (the ground state is $^3\Delta_g$) remains unchanged upon attachment of CO, different from the case for Sc_2.

For the ground state of Ti_2CO, the Ti–Ti bond length is elongated by 0.386 Å relative to the naked Ti_2. The C–O bond length in Ti_2CO is slightly shorter by 0.032 Å than that in Sc_2CO (Figs. 1 and 2). The C–O stretching vibrational frequency in Ti_2CO is calculated to be 1330.9 cm^{-1}, which is in accord with the experimental value of 1297.8 cm^{-1} (Table I) and previous computations.[13] The Ti–C and Ti–O stretching frequencies are predicted to be 719.1, 544.8, and 367.1 cm^{-1} with small intensities of 3, 2, and 2 km/mol (Table II), respectively. The Ti–Ti stretching is predicted to be 256.7 cm^{-1}.

C. V_2CO

The ground state of V_2CO is predicted to be $^3A'$ with a semibridging CO (Fig. 3). Energetically next higher structure with semibridging configuration is calculated to be $^1A'$, which lies 0.8 kcal/mol higher in energy than its ground state. Two low-lying structures with side-on-bonded configurations correspond to the $^3A''$ and $^5A'$ states, respectively, which are above its ground state by 20.0 and 20.5 kcal/mol. The lowest energy terminal configuration is calculated to be an $^5A'$ state with the V–V–C angle of 109.8°, which lies 21.3 kcal/mol higher in energy than its ground state. It is noted that the spin multiplicity of V_2 (the ground state is $^3\Sigma_g^-$) remains unchanged upon attachment of CO, similar to the case for Ti_2 but different from the case for Sc_2.

The V–V bond length in the ground state of V_2CO is slightly shorter by 0.034 Å than that in the naked V_2. The C–O bond length in V_2CO is calculated to 1.184 Å, which is visibly shorter by 0.137 and 0.105 Å than those in Sc_2CO and Ti_2CO (Figs. 1–3), respectively. The C–O stretching vibrational frequency is calculated to be 1825.4 cm^{-1}, which agrees well with the experimental value (1801.6 cm^{-1}) (Table I). The V–V stretching is predicted to be 672.5 cm^{-1}, while its intensity (20 km/mol) is too small to be detected. The V–C stretching frequencies are predicted to be 454.0 and 421.0 cm^{-1} with small intensities of 0.2 and 35 km/mol (Table II), respectively.

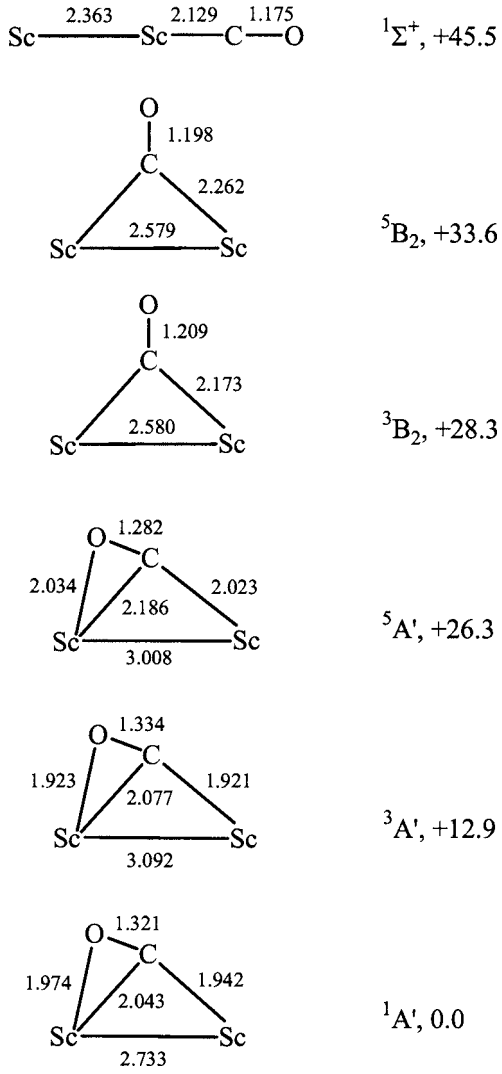

FIG. 1. Representative low-lying structures and their relative energies of Sc_2CO calculated at the BP86/6-311+G(*d*) level of theory (bond length in angstrom, bond angle in degree, and relative energy in kcal/mol).

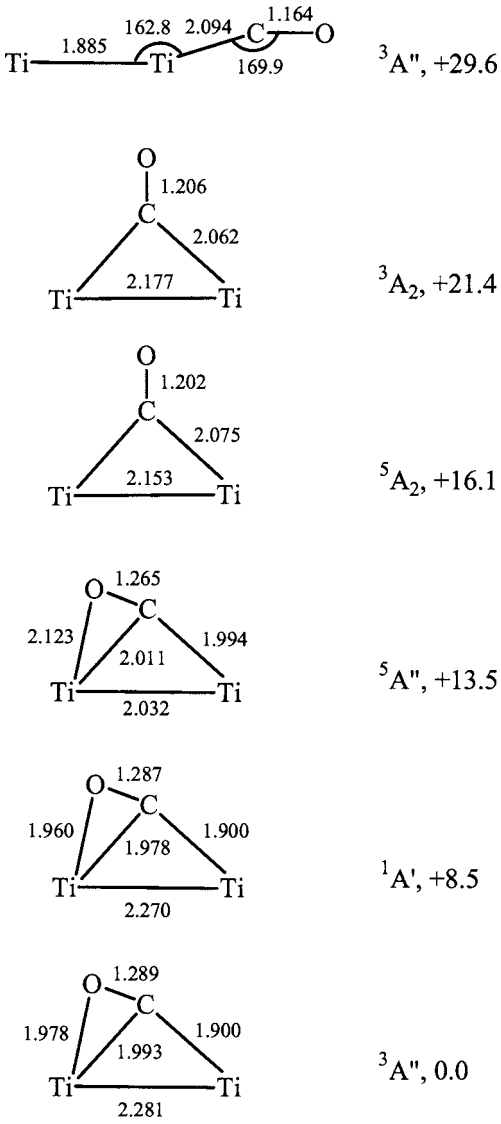

FIG. 2. Representative low-lying structures and their relative energies of Ti_2CO calculated at the BP86/6-311+G(*d*) level of theory (bond length in angstrom, bond angle in degree, and relative energy in kcal/mol).

D. Cr_2CO

The ground state of Cr_2CO is predicted to be $^1A'$ and its geometrical configuration is similar to that of the ground state of V_2CO, where CO is also in the semibridging position (Fig. 4). The lowest $^3A''$ state is separated from the ground state by 1.4 kcal/mol. The lowest energy terminal configuration is calculated to be $^1\Sigma_g^+$, which lies 14.3 kcal/mol higher in energy than the ground state. Other two low-lying bridging and semibridging configurations correspond to the $^3B_1$ and $^5A''$ states, respectively, which are above the ground state by 20.9 and 23.7 kcal/mol. The spin multiplicity of Cr_2 (the ground state is $^1\Sigma_g^+$) remains unchanged upon attachment of CO, similar to the cases for Ti_2 and V_2 but different from the case for Sc_2.

The Cr–Cr bond length in the ground state of Cr_2CO is slightly elongated by 0.047 Å relative to the naked Cr_2. The C–O bond length in Cr_2CO is calculated to 1.162 Å, which is similar to that in V_2CO (1.184 Å) but visibly shorter than those in Sc_2CO (1.321 Å) and Ti_2CO (1.289 Å) (Figs. 1–4). The C–O stretching vibrational frequency is calculated to be 1947.3 cm^{-1}, which should be scaled down by 0.965 to fit the experimental value of 1879.1 cm^{-1} (Table I). The Cr–Cr stretching is predicted to be 710.6 cm^{-1} with small intensity (35 km/mol) (Table II). The Cr–C stretching frequencies are predicted to be 399.1 and 328.0 cm^{-1} with the intensities of 0.1 and 21 km/mol (Table II), respectively.

E. Mn_2CO

The lowest energy geometrical configuration is predicted be a $^9\Sigma^+$ state (Fig. 5). Energetically next higher structure with terminal configuration is calculated to be $^3A''$, which lies 3.1 kcal/mol higher in energy than the $^9\Sigma^+$ state. Two low-lying semibridging and bridging configurations correspond to the $^9A''$ and $^7B_1$ states, respectively, which are above the $^9\Sigma^+$ state by 3.2 and 11.3 kcal/mol. This indicates that the first three low-lying states ($^9\Sigma^+$, $^3A''$, and $^9A''$) are very close in energy. The calculated C–O stretching vibrational frequency in the $^9A''$ state (1763.5 cm^{-1}) is closer to the experimental values [1688.2 and 1687.5 cm^{-1} (Refs. 14 and 15)] than those in the $^9\Sigma^+$ (1902.9 cm^{-1}) and $^3A''$

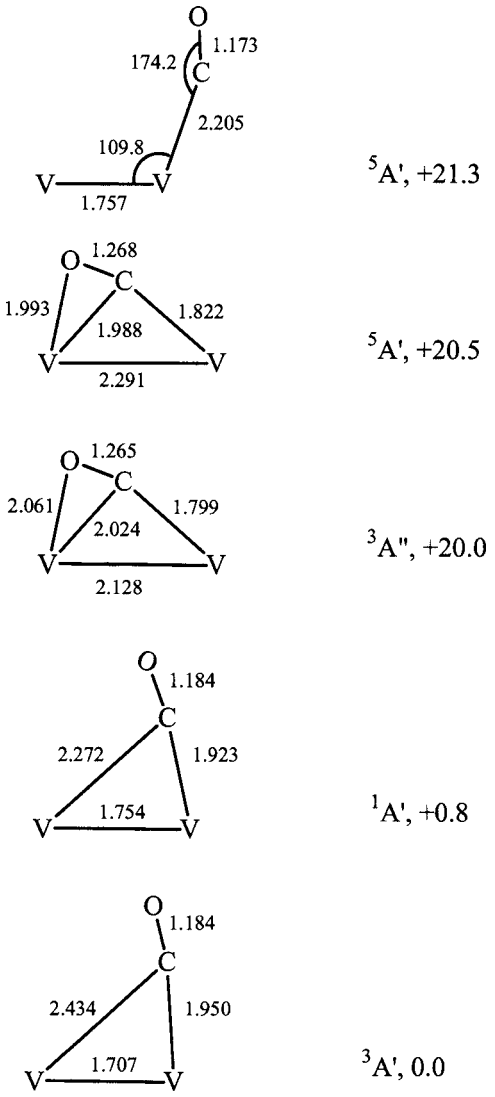

FIG. 3. Representative low-lying structures and their relative energies of V_2CO calculated at the BP86/6-311+G(*d*) level of theory (bond length in angstrom, bond angle in degree, and relative energy in kcal/mol).

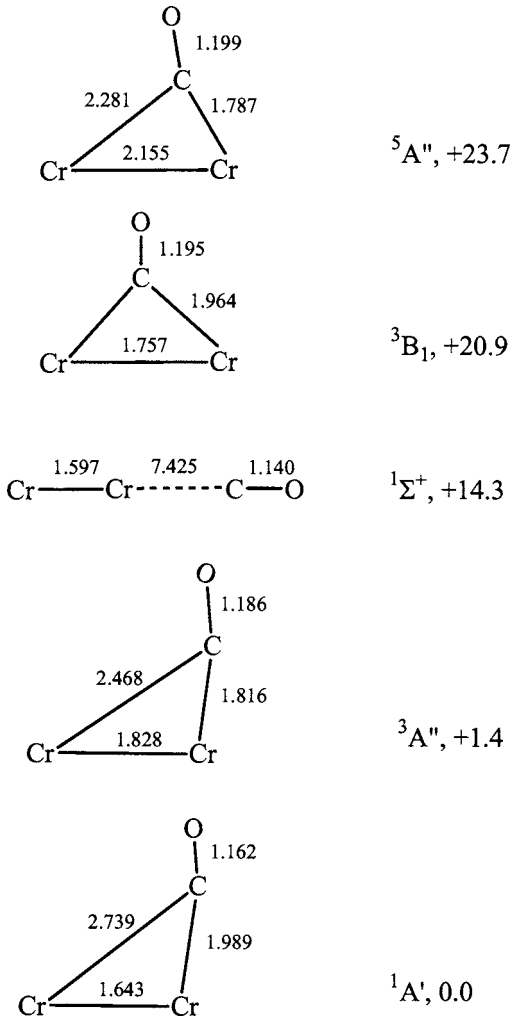

FIG. 4. Representative low-lying structures and their relative energies of Cr_2CO calculated at the BP86/6-311+G(*d*) level of theory (bond length in angstrom, bond angle in degree, and relative energy in kcal/mol).

(1862.1 cm^{-1}) states. For these reasons, the $^9A''$ state is assumed to be the ground state of Mn_2CO. The ground state of naked manganese dimer has been a matter of considerable debate. According to the present computations, the ground state of Mn_2 is $^{11}\Pi_u$, which is consistent with the previous DFT calculations.[40] Some recent investigations claimed that Mn_2 had a $^1\Sigma_g^+$ ground state.[41,42] Anyway, the spin multiplicity of Mn_2 (the ground state is $^1\Sigma_g^+/^{11}\Pi_u$) changes upon attachment of CO, similar to the case for Sc_2 but different from the cases for Ti_2, V_2, and Cr_2.

The Mn–Mn bond length in the ground state of Mn_2CO is elongated by 0.821 Å relative to the $^1\Sigma_g^+$ state of Mn_2 or is shorter by 0.136 Å relative to the $^{11}\Pi_u$ state of Mn_2. The C–O bond length in Mn_2CO is calculated to 1.199 Å, which is similar to those in V_2CO (1.184 Å) and Cr_2CO (1.162 Å) but visibly shorter than those in Sc_2CO (1.321 Å) and Ti_2CO (1.289 Å) (Figs. 1–5). The Mn–C stretching frequencies are predicted to be 507.4 and 321.5 cm^{-1} with small intensities of 5 and 4 km/mol (Table II), respectively. The Mn–Mn stretching frequency is predicted to be 230.2 cm^{-1} with the intensity of 1 km/mol.

F. Fe_2CO and Co_2CO

Detailed discussions about the Fe_2CO and Co_2CO species have been reported previously[18,19] and only the ground state structures and energetically next higher structures of Fe_2CO and Co_2CO are given in Fig. 6. In short, the ground states of Fe_2CO and Co_2CO are predicted to be $^7A'$ and $^5A''$, respectively, where the CO ligands are in the terminal position and the *M*-*M*-C angles (*M*=Fe,Co) are 119.8° and 117.0° (Fig. 6). Energetically next higher structures for Fe_2CO and Co_2CO are calculated to be $^5A'$ and $^3A''$, respectively, where the CO ligands are in the semibridging position between the two metal atoms. The C–O stretching vibrational frequencies in the ground states of Fe_2CO and Co_2CO are calculated to be 1927.3 and 1958.3 cm^{-1}, respectively, which agree well with the experimental values (1898.0 and 1953.3 cm^{-1}) (Table I). Our computations are consistent with the previous reports.[16–19,21]

G. Ni_2CO

The ground state of Ni_2CO is predicted to be $^1A_1$, where CO is in the bridging position between the two nickel atoms (Fig. 7). Energetically next higher structure corresponds to

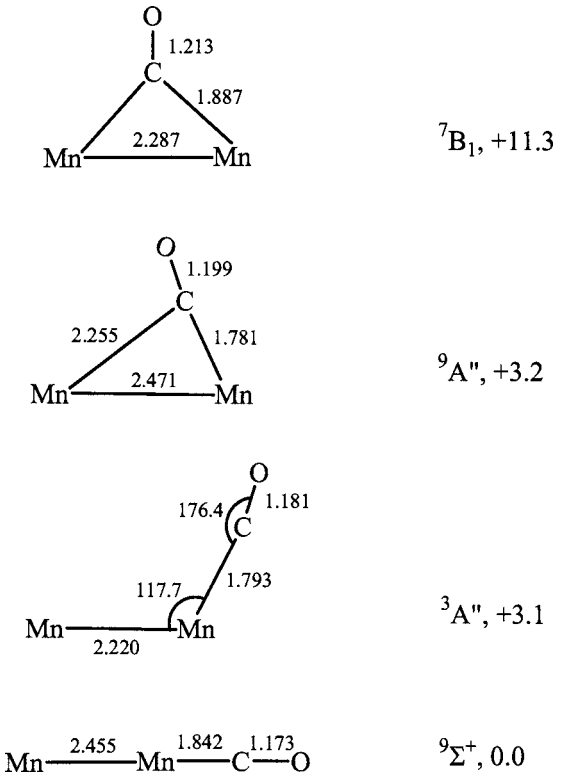

FIG. 5. Representative low-lying structures and their relative energies of Mn_2CO calculated at the BP86/6-311+G(*d*) level of theory (bond length in angstrom, bond angle in degree, and relative energy in kcal/mol).

an $^3A''$ state, which is above its ground state by 10.8 kcal/mol. The $^3A''$ state of Ni_2CO carries a terminal CO with the Ni–Ni–C angle of 144.6°. The structure with the linear configuration lies 11.1 kcal/mol higher in energy than the ground state and has one imaginary frequency (the structure is not shown here), which is consistent with the previous computation.[22] The ground state of naked nickel dimer is still the subject of discussions. The present computations predict the ground state of Ni_2 to be $^3\Sigma_g^-$, which is in accord with the previous DFT computations.[40] The spin multiplicity of Ni_2 (the ground state is $^3\Sigma_g^-$) changes upon attachment of CO, similar to the cases for Sc_2 and Mn_2 but different from the cases for Ti_2, V_2, Cr_2, Fe_2, and Co_2.

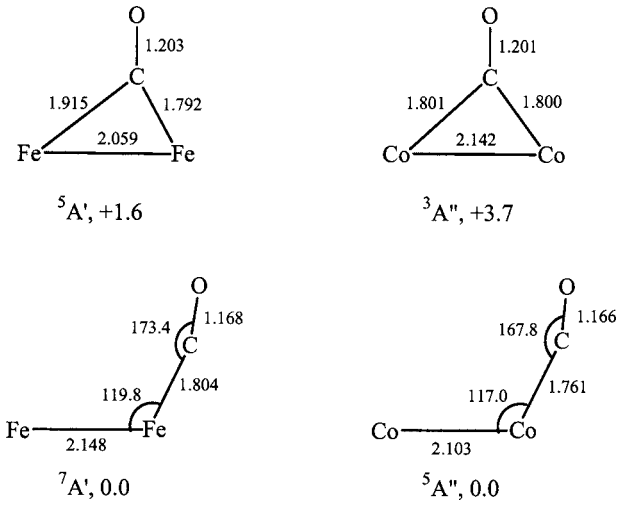

FIG. 6. Ground state structures and energetically next higher isomers for Fe_2CO and Co_2CO calculated at the BP86/6-311+G(*d*) level of theory (bond length in angstrom, bond angle in degree, and relative energy in kcal/mol).

The Ni–Ni bond length in the ground state of Ni_2CO is slightly elongated by 0.151 Å relative to the naked Ni_2. The C–O bond length in Ni_2CO is calculated to 1.196 Å, which is similar to those in M_2CO (M=V, Cr, Mn, Fe, Co) (1.162–1.184 Å) but visibly shorter than those in M_2CO (M=Sc,Ti) (1.289–1.321 Å) (Figs. 1–7). The C–O stretching vibrational frequency in Ni_2CO is calculated to be 1793.0 cm^{-1}, which agrees well with the experimental value (1769.1 cm^{-1}) (Table I). The Ni–Ni stretching is predicted to be 266.4 cm^{-1} with very weak intensity (0.4 km/mol) (Table II).

H. Cu_2CO

Cu_2CO has a $^1\Sigma^+$ ground state with a terminal CO (Fig. 7), which is in agreement with the previous computations.[24,25(a)] The lowest energy bridging configuration corresponds to an $^1A_1$ state, which is above its ground state by 26.7 kcal/mol. Recent DFT calculations using the effective core potential plus double zeta basis set for copper atom showed that the ground state of Cu_2CO has a bent and terminal CO.[25(b)] Using the Wachters–Hay all-electron basis set for copper atoms, however, optimizations performed beginning with bent trial geometries all have arrived at linear configurations, suggesting a basis set effect on the geometrical configuration of the ground state of Cu_2CO. Such effect of basis set has not been found for other 3*d* metals. It is noted that the spin multiplicity of Cu_2 (the ground state is $^1\Sigma_g^+$) remains unchanged upon attachment of CO, similar to the cases for Ti_2, V_2, Cr_2, Fe_2, and Co_2 but different from the cases for Sc_2, Mn_2, and Ni_2.

The Cu–Cu bond length in the ground state of Cu_2CO is slightly elongated by 0.008 Å relative to the naked Cu_2. The C–O bond length in Cu_2CO is calculated to 1.148 Å, which is similar to those in M_2CO (M=V to Ni) (1.162–1.184 Å) but visibly shorter than those in M_2CO (M=Sc,Ti) (1.289–1.321 Å) (Figs. 1–7). The C–O stretching vibrational frequency is calculated to be 2071.1 cm^{-1}, which is consistent with the experimental observations (Table I). The Cu–C stretching is predicted to be 425.8 cm^{-1} with very weak intensity of 0.01 km/mol (Table II).

I. Zn_2CO

Zn_2CO has an $^1A'$ ground state with a semibridging CO (Fig. 7). The lowest energy terminal configuration corresponds to an $^3A''$ state, which is above its ground state by 35.5 kcal/mol. The spin multiplicity of Zn_2 (the ground state is $^1\Sigma_g^+$) remains unchanged upon attachment of CO, similar to the cases for Ti_2, V_2, Cr_2, Fe_2, Co_2, and Cu_2 but different from the cases for Sc_2, Mn_2, and Ni_2. The Zn–Zn bond length in the ground state of Zn_2CO is slightly shorter by 0.003 Å relative to the naked Zn_2. The Zn–C bond length is ~7.8 Å and the C–O bond length of 1.140 Å is the same as the value of the free CO molecule calculated at the same

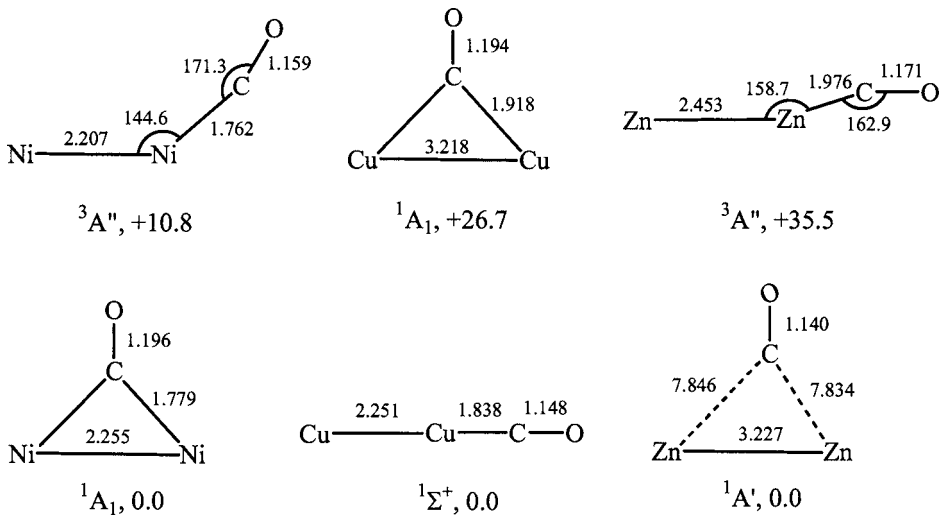

FIG. 7. Ground state structures and energetically next higher isomers Ni_2CO, Cu_2CO, and Zn_2CO calculated at the BP86/6-311+G(*d*) level of theory (bond length in angstrom, bond angle in degree, and relative energy in kcal/mol).

level of theory. This suggests that CO is unbound with the zinc dimer, which is consistent with the absence of Zn_2CO from experiments.

IV. TREND ANALYSIS

The low-lying structures and their relative energies together with vibrational frequencies of M_2CO (M=Sc to Zn) have been discussed in the above sections. We turn now to general trends in the interaction of carbon monoxide with 3*d* metal dimers. It is generally found that on going from left to right across the 3*d* series, the preference for geometrical configuration is from side-on-bonded mode to bridging, and then to terminal, whereas Ni_2CO adopts bridging mode. The C–O stretching vibrational frequencies in the ground states of M_2CO increase generally from the left to the right side of 3*d* metals. The binding energies are predicted to be 68.6 (Sc), 49.5 (Ti), 29.1 (V), 14.3 (Cr), (Mn), 32.2 (Fe), 38.9 (Co), 49.1 (Ni), 27.7 (Cu), and 0.01 kcal/mol (Zn), respectively, showing an overall decreasing trend. As illustrated in Fig. 8, the HOMOs of M_2CO (M=Sc,Ti) are π-type bond, which comprise the metal→CO 2π backbonding, leading to the weakening of the C–O bond. The HOMOs of M_2CO (M=V to Cu) are nonbonding and the HOMO-1s for V, Cr, and Co comprise the metal→CO 2π backbonding. There is no obvious interaction of CO with Zn_2, as shown in Fig. 8.

These general trends can be understood by considering the metal-CO bonding mechanism. This is the familiar synergistic combination of CO 5σ electron donation into the metal valence bands with a compensating backdonation into the CO $2\pi^*$ antibonding molecular orbital. The 3*d* orbital of the metal atoms decreases in size as one goes from left to right in the Periodic Table, which leads to a decrease of $d\pi$ backdonation. This corresponds to a stronger C–O bond and therefore to a higher C–O stretching vibrational frequency. Perusal of the data of adiabatic ionization energies in Table III reveals that on going from left to right in the Periodic Table, the possibility of losing an electron from the metal dimer grows down, implying that CO will gain more electrons from Sc_2 and Ti_2 than the others. The values of Mulliken atomic charges for M_2CO support this conclusion (Table IV).

The above trends in the interaction of carbon monoxide with 3*d* metal dimers mirror the main features of the adsorption of carbon monoxide on transition metal surfaces. In general, dissociation adsorption of CO is suppressed on going from left to right in the Periodic Table of 3*d* metal elements.[1–8] Chemisorption and dissociation of CO occur on early transition metal surfaces and side-on-bonded CO is more stable than the terminally bonded CO as were found in some surfaces.[4] CO adsorbs in a terminal orientation with the carbon end toward the surfaces to the right side of 3*d* series, such as Co, Ni, and Cu.[5–8] It should be noted that surface defects such as steps and kinks can also facilitate CO dissociation on some transition metals including those to the right side of the transition series.[3] Thus, our present computations together with the recent reports[9–25] model the adsorption and dissociation of CO on transition metal surfaces, especially offering the geometrical configurations for the unusually low

TABLE III. Calculated (BP86) and experimental adiabatic ionization energies (kcal/mol) of the naked 3*d* metal dimers.

Species	Sc_2	Ti_2	V_2	Cr_2	Mn_2	Fe_2	Co_2	Ni_2	Cu_2	Zn_2
Calc.	121.8	140.5	148.3	191.5	147.1	159.8	169.2	181.8	190.7	180.2
Expt.	···	···	146.6[a]	161.4[b]	⩽149.2[c]	145.3[d]	⩽148.1[e]	171.3[f]	182.2[g]	207.5[h]

[a]Reference 43.
[b]Reference 44.
[c]Reference 45.
[d]Reference 46.
[e]Reference 47.
[f]Reference 48.
[g]Reference 49.
[h]Reference 50.

TABLE IV. Mulliken atomic charges of the ground state M_2CO (M=Sc to Zn) species calculated at the BP86/6-311+G(d) level of theory.

Species	Sc_2CO	Ti_2CO	V_2CO	Cr_2CO	Mn_2CO	Fe_2CO	Co_2CO	Ni_2CO	Cu_2CO	Zn_2CO
M_2	0.624	0.493	0.290	0.061	0.085	0.048	0.066	0.112	−0.457	0.000
C	−0.305	−0.322	−0.088	0.057	0.180	0.097	0.038	0.030	0.393	−0.041
O	−0.229	−0.171	−0.202	−0.118	−0.265	−0.145	−0.104	−0.142	0.064	0.041

observed C–O stretching frequencies (1100–1400 cm^{-1}) of the chemisorbed CO molecules on transition metal surfaces and metal catalysts.[1–8]

V. CONCLUSIONS

The equilibrium geometries and harmonic vibrational frequencies of the possible structures and electronic states of M_2CO (M=Sc to Zn) were determined using six different exchange-correlation density functionals. All the configurations are found to be planar. The geometry optimization procedures starting with nonplanar trial structures without imposing any symmetry constraint all resulted in the planar configurations. The computed results agree with the available experimental observations and previous theoretical studies. The BP86 functional gives calculated C–O stretching vibrational frequencies much closer to the experimental values than the B3P86, B3LYP, mPW1PW91, and PBE1PBE functionals. It is noted that replacing the correlation part by the LYP correlation functional yields essentially the same results.

It is generally found that on going from left to right across the 3d series, the preference for bonding mode of CO to the metal dimer is from side-on bonded to bridging, and then to terminal, whereas Ni_2CO prefers bridging configuration. The C–O stretching vibrational frequencies in the ground states of M_2CO increase generally from the left to the right side of 3d metals. The binding energies exhibit an overall decreasing trend. These general trends in the interaction of carbon monoxide with 3d metal dimers mirror the main features of the adsorption of carbon monoxide on transition metal surfaces. Most importantly, we hope our work would stimulate systematically theoretical studies on the interaction of small molecules (i.e., CO_2, H_2, H_2O, CH_4, C_2H_4, etc.) with a series of metal clusters at consistent levels of theory with the goal to understand the multifaceted mechanisms of the adsorption of such molecules on metal surfaces and catalysts.

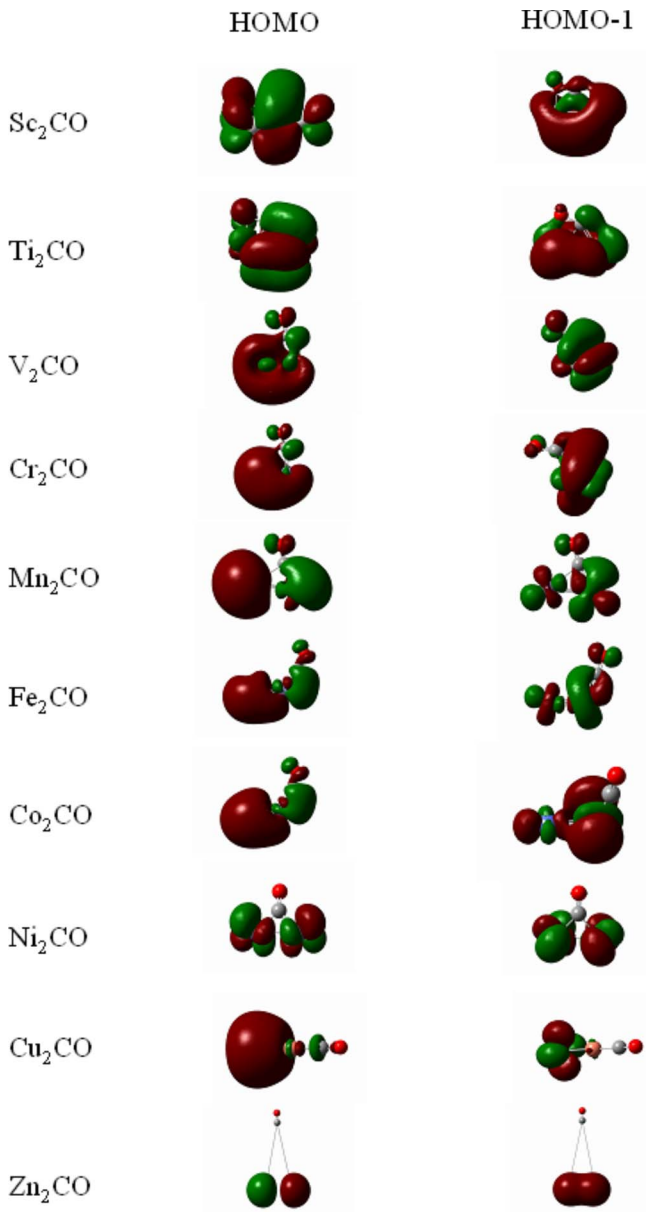

FIG. 8. (Color online) Molecular orbital depictions of the HOMOs and HOMO-1s of the ground state of M_2CO (M=Sc to Zn) species.

ACKNOWLEDGMENTS

This work was supported by AIST and a Grant-in-Aid for Scientific Research (B) (Grant No. 17350012) from the Ministry of Education, Culture, Sports, Science and Technology (MEXT) of Japan. L.J. is grateful to JSPS for a postdoctoral fellowship.

[1] *The Nature of the Surface Chemical Bond*, edited by T. N. Rhodin and G. Ertl (North-Holland, Amsterdam, 1979); *The Chemical Physics of Solid Surfaces and Heterogeneous Catalysis*, edited by D. A. King and D. P. Woodruff (Elsevier, Amsterdam, 1991); *Advanced Inorganic Chemistry*, 6th ed., edited by F. A. Cotton, G. Wilkinson, C. A. Murillo, and M. Bochmann (Wiley, New York, 1999).
[2] M. A. Vannice, Catal. Today **12**, 255 (1992); E. I. Solomon, P. M. Jones, and J. A. May, Chem. Rev. (Washington, D.C.) **93**, 2623 (1993); A. Sen, Acc. Chem. Res. **26**, 303 (1993).
[3] See, for example, *Introduction to Surface Chemistry and Catalysis*, edited by G. A. Somorjai (Wiley, New York, 1994); A. C. Pavão, T. C. Guimarães, S. K. Lie, C. A. Taft, and W. A. Lester, Jr., J. Mol. Struct.: THEOCHEM **458**, 99 (1999) and references therein; Z. P. Liu and P. Hu, J. Am. Chem. Soc. **125**, 1985 (2003); P. Crawford and P. Hu, J. Chem. Phys. **126**, 194706 (2007).
[4] N. D. Shinn and T. E. Madey, Phys. Rev. Lett. **53**, 2481 (1984); N. D. Shinn and T. E. Madey, J. Chem. Phys. **83**, 5928 (1985); D. W. Moon, S. L. Bernasek, D. J. Dwyer, and J. L. Gland, J. Am. Chem. Soc. **107**, 4363

(1985).
[5] S. L. Tang, J. D. Beckerle, M. B. Lee, and S. T. Ceyer, J. Chem. Phys. **84**, 6488 (1986).
[6] H. P. Steinruch, A. Winkler, and K. D. Rendulic, Surf. Sci. **152**, 323 (1985).
[7] M. A. Hines and R. N. Zare, J. Chem. Phys. **98**, 9134 (1993).
[8] D. Heskett, E. W. Plummer, and R. P. Messmer, Surf. Sci. **139**, 558 (1984).
[9] L. Jiang and Q. Xu, J. Am. Chem. Soc. **127**, 42 (2005); J. Phys. Chem. A **110**, 5636 (2006).
[10] Q. Xu, L. Jiang, and R. Q. Zou, Chem.-Eur. J. **12**, 3226 (2006).
[11] M. F. Zhou, X. Jin, and J. Li, J. Phys. Chem. A **110**, 10206 (2006).
[12] X. Jin, L. Jiang, Q. Xu, and M. F. Zhou, J. Phys. Chem. A **110**, 12585 (2006).
[13] Q. Xu, L. Jiang, and N. Tsumori, Angew. Chem., Int. Ed. **44**, 4338 (2005).
[14] H. Huber, E. P. Kundig, G. A. Ozin, and A. J. Poe, J. Am. Chem. Soc. **97**, 308 (1975).
[15] L. Andrews, M. F. Zhou, X. F. Wang, and C. W. Bauschlicher, Jr., J. Phys. Chem. A **104**, 8887 (2000).
[16] M. F. Zhou, G. V. Chertihin, and L. Andrews, J. Chem. Phys. **109**, 10893 (1998).
[17] M. F. Zhou and L. Andrews, J. Chem. Phys. **110**, 10370 (1999).
[18] B. Tremblay, G. Gutsev, L. Manceron, and L. Andrews, J. Phys. Chem. A **106**, 10525 (2002).
[19] B. Tremblay, L. Manceron, G. Gutsev, L. Andrews, and H. Partridge III, J. Chem. Phys. **117**, 8479 (2002).
[20] M. Moskovits and J. E. Hulse, J. Phys. Chem. **81**, 2004 (1977).
[21] G. L. Gutsev, C. W. Bauschlicher, Jr., and L. Andrews, J. Chem. Phys. **119**, 3681 (2003).
[22] I. S. Ignatyev, H. F. Schaefer III, R. B. King, and S. T. Brown, J. Am. Chem. Soc. **122**, 1989 (2000).
[23] D. Post and E. J. Baerends, J. Chem. Phys. **78**, 5663 (1983).
[24] P. Fournier, J. Chem. Phys. **102**, 5396 (1995).
[25] (a) Q. S. Li, Y. D. Liu, Y. M. Xie, R. B. King, and H. F. Schaefer III, Inorg. Chem. **40**, 5842 (2001); (b) Z. X. Cao, Y. J. Wang, J. Zhu, W. Wu, and Q. E. Zhang, J. Phys. Chem. B **106**, 9649 (2002).
[26] M. J. Frisch, G. W. Trucks, H. B. Schlegel *et al.*, GAUSSIAN03, Revision B.04, Gaussian Inc., Pittsburgh, PA, 2003.
[27] A. D. McLean and G. S. Chandler, J. Chem. Phys. **72**, 5639 (1980); R. Krishnan, J. S. Binkley, R. Seeger, and J. A. Pople, *ibid.* **72**, 650 (1980).
[28] A. J. H. Wachter, J. Chem. Phys. **52**, 1033 (1970).
[29] P. J. Hay, J. Chem. Phys. **66**, 4377 (1977).
[30] A. D. Becke, Phys. Rev. A **38**, 3098 (1988).
[31] A. D. Becke, J. Chem. Phys. **98**, 5648 (1993).
[32] J. P. Perdew, Phys. Rev. B **33**, 8822 (1986).
[33] J. P. Perdew, Phys. Rev. B **34**, 7046 (1986).
[34] C. Lee, E. Yang, and R. G. Parr, Phys. Rev. B **37**, 785 (1988).
[35] C. Adamo and V. Barone, J. Chem. Phys. **108**, 664 (1998).
[36] J. P. Perdew, K. Burke, and M. Ernzerhof, Phys. Rev. Lett. **78**, 1396 (1997).
[37] J. P. Perdew and Y. Wang, Phys. Rev. B **45**, 13244 (1992).
[38] M. F. Zhou, L. Andrews, and C. W. Bauschlicher, Jr., Chem. Rev. (Washington, D.C.) **101**, 1931 (2001) and references therein.
[39] H. J. Himmel, A. J. Downs, and T. M. Greene, Chem. Rev. (Washington, D.C.) **102**, 4191 (2002) and references therein.
[40] G. L. Gutsev and C. W. Bauschlicher, Jr., J. Phys. Chem. A **107**, 4755 (2003).
[41] S. Yanagisawa, T. Tsuneda, and K. Hirao, J. Chem. Phys. **112**, 545 (2000); C. J. Barden, J. C. Rienstra-Kiracofe, and H. F. Schaefer III, *ibid.* **113**, 690 (2000).
[42] J. R. Lombardi and B. Davis, Chem. Rev. (Washington, D.C.) **102**, 2431 (2002) and references therein.
[43] A. M. James, P. Kowalczyk, E. Langlois, M. D. Campbell, A. Ogawa, and B. Simard, J. Chem. Phys. **101**, 4485 (1994).
[44] B. Simard, M. A. Lebeault-Dorget, A. Marijnissen, and J. J. ter Meulen, J. Chem. Phys. **108**, 9668 (1998).
[45] M. F. Jarrold, A. J. Illies, and M. T. Bowers, J. Am. Chem. Soc. **107**, 7339 (1985).
[46] E. A. Rohlfing, D. M. Cox, A. Kaldor, and K. H. Johnson, J. Chem. Phys. **81**, 3846 (1984).
[47] D. A. Hales, C. X. Su, L. Lian, and P. B. Armentrout, J. Chem. Phys. **100**, 1049 (1994).
[48] J. C. Pinegar, J. D. Langenberg, C. A. Arrington, E. M. Spain, and M. D. Morse, J. Chem. Phys. **102**, 666 (1995).
[49] A. S. Sappey, J. E. Harrington, and J. C. Weisshaar, J. Chem. Phys. **91**, 3854 (1989).
[50] S. W. Buckner, J. R. Gord, and B. S. Freiser, J. Chem. Phys. **88**, 3678 (1988).